Articles

2013-04-01

Thermal Performance Analysis of a Solar Water Heating System With Heat Pipe Evacuated Tube Collector Using Data From a Field Trial

Lacour Ayompe
Technological University Dublin, lacour.ayompe@tudublin.ie

Aidan Duffy
Technological University Dublin, aidan.duffy@tudublin.ie

Recommended Citation

Thermal performance analysis of a solar water heating system with heat pipe evacuated tube collector using data from a field trial

L.M. Ayompe[1] and A. Duffy
School of Civil & Building Services Engineering and Dublin Energy Lab, Dublin Institute of Technology, Dublin 1, Ireland.

Abstract

This paper presents an analysis of the thermal performance of a solar water heating system with heat pipe evacuated tube collector using data obtained from a field trial installation over a year in Dublin, Ireland. An automated sub-system was developed and incorporated to control the hot water draw-offs and electric immersion heater to mimic the operation of solar water heating systems in domestic dwellings. The maximum recorded collector outlet fluid temperature was 70.3^{o}C while the water temperature at the bottom of the hot water tank was 59.5^{o}C. The annual average daily energy collected was 20.4 MJd^{-1}, energy delivered by the solar coil was 16.8 MJd^{-1}, supply pipe loss was 3.6 MJd^{-1}, solar fraction was 33.8%, collector efficiency was 63.2% and system efficiency was 52.0%. Reducing the supply pipe losses which represented 17.7% of energy collected and 21.5% of energy delivered to the hot water tank, and developing a better pump control strategy for heavily overcast and intermittent cloud covered days could result in system improvement.

Keywords: Solar water heating system, heat pipe, evacuated tube collector.

1.   Introduction

Evacuated tube collectors (ETCs) consist of glass vacuum-sealed tubes with the absorber surface located in the inner glass tube having different shapes. ETCs may be subdivided in two types: 'direct flow through' (or 'water-in-glass') and 'heat pipe'. Direct flow through ETCs consist of a set of glass tubes connected to a tank or shell. A larger

---

[1] Corresponding author: Email address: lacour.ayompe@dit.ie (L.M. Ayompe); Tel: +353 14027937

diameter glass tube is used to surround each tube with the annular space between the tubes evacuated to reduce heat losses. The heat transfer liquid is heated as it circulates in the tubes (Zambolin and Del Col, 2010, Morrison et al., 2004).

A heat pipe (HP) consists of tubes of high thermal conductance which are sealed and contain a small amount of working fluid. The heat is transferred as latent heat energy by evaporating the working fluid in a heating zone and condensing the vapour in a cooling zone, the circulation is completed by return flow of the condensate to the heating zone through the capillary structure which lines the inner wall of the container (Dunn and Reay, 1982, Faghri, 1995). The tubes are mounted with the metal tips projecting into a heat exchanger (manifold) containing flowing water or water/glycol. Heat is transferred into the manifold and through circulation pipework to be used in heating and/or hot water applications.

A heat pipe evacuated tube collector (HP-ETC) consists of a heat pipe inside a vacuum-sealed tube. The vacuum envelope reduces convection and conduction losses, so the collectors can operate at higher temperatures than flat plate collectors (FPCs). Like FPCs, HP-ETCs collect both direct and diffuse radiation. They have higher efficiency at low incidence angles giving them an advantage over FPC in day-long performance (Kalogirou, 2004). Typically heat-absorbing fins are attached to the tubes to maximise thermal gains.

The main difference in thermal performance between a HP-ETC and conventional HP technologies lies in the heat transfer processes from the absorber tube wall to the energy transporting fluid. In the HP-ETC the processes involved are evaporation, condensation and convection, whereas for conventional HP solar collectors, heat transfer occurs only in the absorber plate. Solar collectors with HPs have lower thermal masses, resulting in a faster response times (Riffat *et al.*, 2005).

HPs operate like a thermal diode, i.e., with unidirectional heat flow. This minimizes heat loss from the transporting fluid when incident radiation is low. Furthermore, when the maximum design temperature of the collector is reached, additional heat transfer can be prevented. This prevents over-heating of the circulating fluid, a common problem in many solar collector systems (de Vries et al., 1980).

The use of HP-ETCs in solar water heating systems (SWHSs) is increasing worldwide because of their high thermal efficiencies and operating water temperatures when compared to flat plate collectors (FPCs). However, the on-site thermal performance of SWHSs with evacuated tube collectors has not been well evaluated and is therefore not well known to users (Chow et al., 2011).

Few researchers have evaluated the thermal performance of SWHSs with ETCs both experimentally and theoretically. Houri et al. (2013) measured the energy produced from a thermosyphon SWHS with an evacuated tube collector in an inhabited domestic dwelling in Lebanon. Redpath (2012) evaluated the performance of three proprietary thermosyphon heat-pipe evacuated tubes solar water heaters using hot water heating loads of three domestic dwelling types in a northern maritime climate. Hayek et al. (2011) carried out an experimental investigation of the performance of two forced circulation SWHSs with water-in-glass and HP-ETC under Eastern Mediterranean climatic conditions. Chow et al. (2011) evaluated the year round thermal performance of a single-phase open thermosyphon and two-phase closed thermosyphon SWHSs with ETCs for domestic hot water applications under Hong Kong weather conditions. Zambolin and Del Col (2010) carried out a comparative performance analysis of the thermal performance of flat plate and evacuated tube collectors in stationary standard and daily conditions in Padova, Italy.

Building Research Establishment (2009) evaluated the performance of a solar water heating system in Cambridgeshire, UK which had a flat plate solar panel (Clearline V30)

manufactured by Viridan Solar, UK. The test rig included an automated system that incorporated the effects of the auxiliary heating system (boiler or immersion heater) and daily hot water use of the average European household described by the EU reference tapping cycle (EU M324EN) equivalent to 100 litres at 60°C. Their results showed that over a year, the 3 m^2 solar panel generated 5,266 MJ of heat accounting for 57% of the hot water requirement.

The above mentioned studies except that by Building Research Establishment (with a flat plate collector) were either carried out on thermosyphon SWHSs or forced circulation systems in locations with climatic conditions different from those typical of northern European countries. Also the papers do not present information on the detailed performance of the individual components of the SWHSs. As a result they do not provide information on how the solar fluid flow rate, water temperature inside the hot water tank, and energy collection vary under different weather conditions.

This paper therefore presents results of the analysis of the thermal performance of a SWHS with 3 m^2 HP-ETC using data from a field trial in Dublin, Ireland. The SWHS is typical of systems installed in average sized single domestic dwellings in Ireland with 4-6 inhabitants. An automated system was developed and incorporated to control hot water draw-offs to mimic the demand for hot water in domestic dwellings. An electric immersion heater was incorporated to provide 'top-up' energy when insufficient solar radiation was available, as is typical in Ireland and the UK. The data collected were used to evaluate energy performance indices notably: system component temperatures, collector energy outputs; energy delivered to the hot water tank; collector and system efficiencies; pipework heat loss; and solar fraction on daily, monthly and yearly basis.

2. Methodology

A forced circulation SWHS with 3 m^2 HP-ETC was installed on a flat rooftop in the Focas Institute, Dublin, Ireland (latitude 53° 20' N and longitude 6° 15') and its thermal performance was monitored over a one year period. The SWHS had a 300 litre hot water tank equipped with an electrical auxiliary immersion heater which was used to top up the tank temperature to 60°C in the morning and evening whenever the solar coil fell short of doing so. An automated hot water draw off system was developed to mimic domestic hot water use (volumetric flow rates are shown in Fig. 1). System performance data were collected every minute.
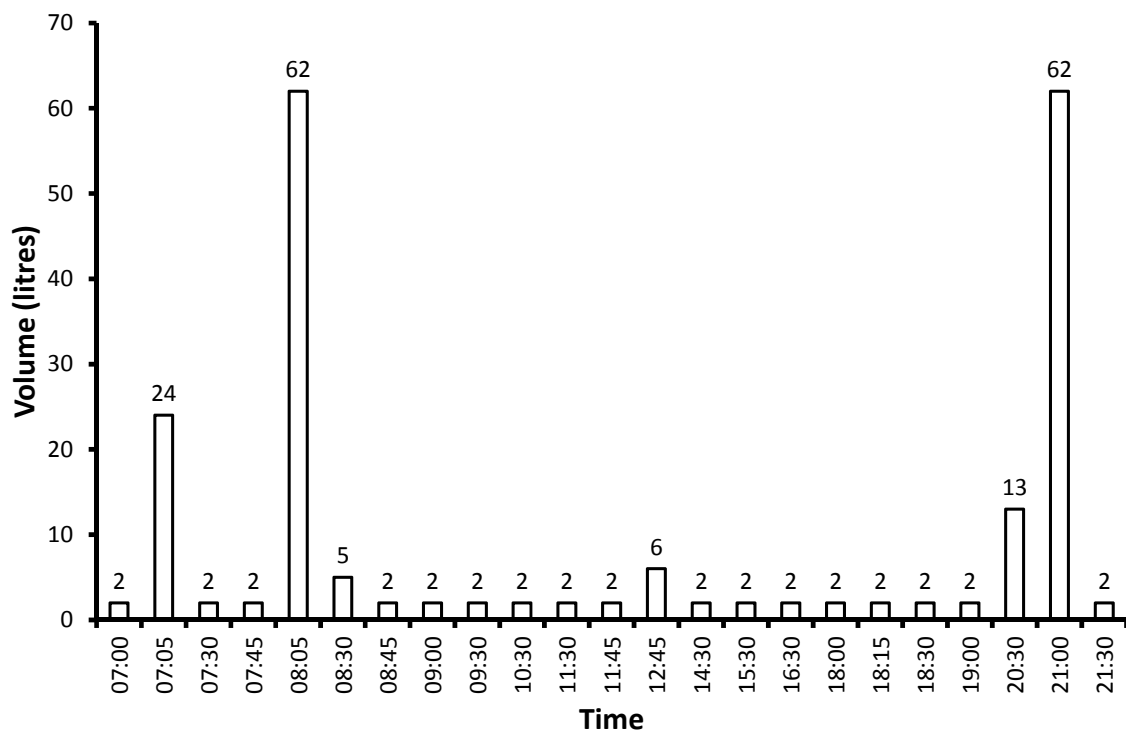
Fig. 1. Volume of hot water (60°C) draw-off at different times of the day.

2.1. System description

Typical solar water heating systems used in temperate climates consist of a hot water storage tank, control unit, pump station and either flat plate or evacuated tube collectors. The HP-ETC employed in this study was south facing and inclined at 53°, equal to the local latitude of the location. The hot water tank was installed nearby in the building's plant room. The solar circuits consisted of 12 mm diameter (outside) copper pipes insulated with 22 mm thick Class O Armaflex. All pipe fittings were insulated to reduce heat losses. The solar circuit pipe length supply and return were 14 m and 15.4 m respectively.

The collector was a Thermomax HP200 consisting of a row of 30 evacuated heat pipe tubes and an insulated water manifold. It had two separate circuits, one in each individual tube inside the heat pipe and one in the manifold through which the solar fluid circulates. The collector had a total collector plate (absorber) surface of 3 m^{2} and the tubes had a vacuum level of 10^{-5} mbar based on the manufacturer's specifications. Fig. 2 shows pictures of the Thermomax HP200 collector and details of the heat pipe tubes and manifold.
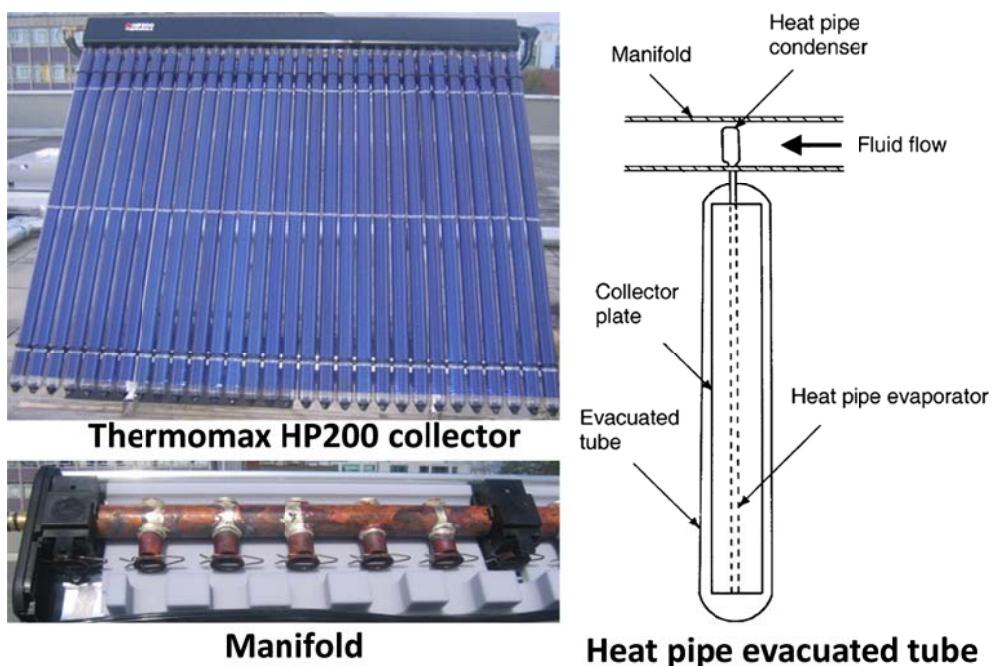
Fig. 2. Thermomax HP200 collector, heat pipe evacuated tubes and manifold.

6

The stainless steel hot water tank (model HM 300L D/coil U44332) was 1,680 mm high with a diameter of 580 mm and an operating pressure of 3 bar. The tank was equipped with an electric immersion heater of 2.75/3.0 kW capacity located at the middle of the tank. The tank had a heating coil with surface area of 1.4 m^2 and a rating of 21 kW.

The hot water demand profile employed was the EU reference tapping cycle number 3 (see Fig. 1), equivalent to a daily energy output of 42.1 MJ representing 199.8 litres of water at 60°C. It is based on hot water use of the average European household described in the European Union mandate for the elaboration and adoption of measurement standards for household appliances EU M324EN (European Commission, 2002).

An automated hot water dispensing unit was designed and incorporated into the SWHS to draw-off water from the hot water tank in such a way as to mimic real life operation by households. The unit includes a programmable logic controller (PLC), contactors, relays, electrical fittings, solenoid valve, thermostat and impulse flow meters. A software program was written to control the auxiliary heating system as well as opening and shutting the solenoid valves.

Fig. 3 shows a flow chart of the daily operation of the PLC. The PLC turned on the immersion heater at the middle of the hot water tank between 5-8 am and 6-9 pm daily just before the two peak hot water draw-offs to ensure that hot water was available when needed. An analogue thermostat placed at the top of the hot water tank was set to turn off the electricity supply to the immersion heater when the temperature of the water at the top of the tank exceeded 60°C. Hot water was dispensed using a solenoid valve that was opened and closed using signals from the PLC. A pulse flow meter (1 pulse per litre) installed at the end of the solenoid valve was used to count the number of litres of water extracted from

7

the hot water tank. The solenoid valve was closed when the required volume of water was dispensed based on the water demand profile (see Fig. 1).

Fig. 4 shows a schematic diagram of the experimental setup of the SWHS components and the position of the thermocouple sensors. Parameters measured include the following: solar fluid temperature at the collector outlet ($T_{c,o}$), water temperature at the bottom of the hot water tank ($T_{b,t}$), water temperature at the middle of the hot water tank ($T_{m,t}$), solar fluid temperature at inlet to the solar coil ($T_{sc,i}$), solar fluid temperature at the outlet from the solar coil ($T_{sc,o}$), solar fluid temperature at inlet to the collector ($T_{c,i}$), cold water inlet temperature to the hot water tank ($T_{cw,i}$), hot water supply temperature ($T_{hw,o}$) and the volume flow rate of the solar fluid.
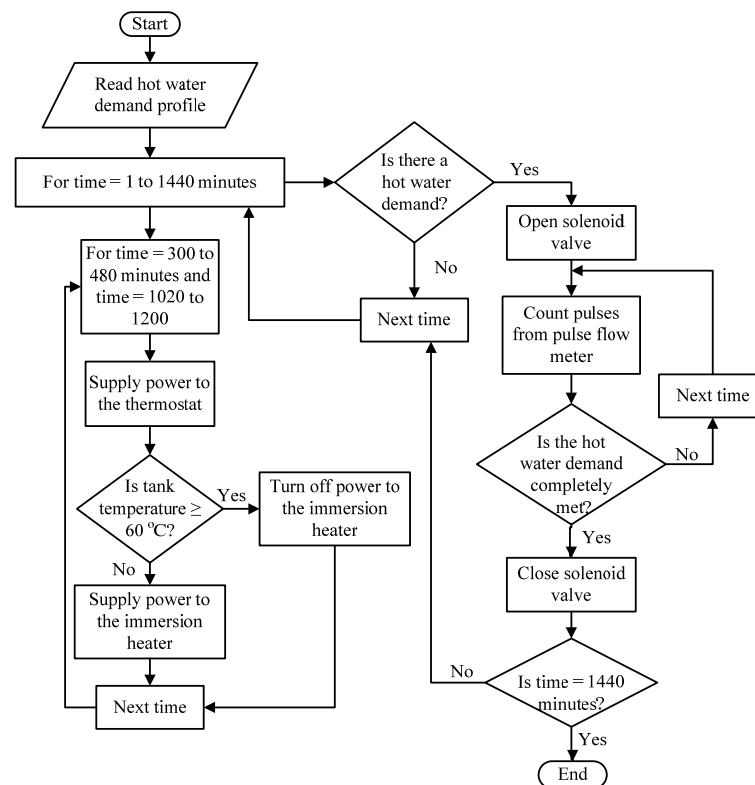
Fig. 3. Flow chart of the daily operation of the PLC

8
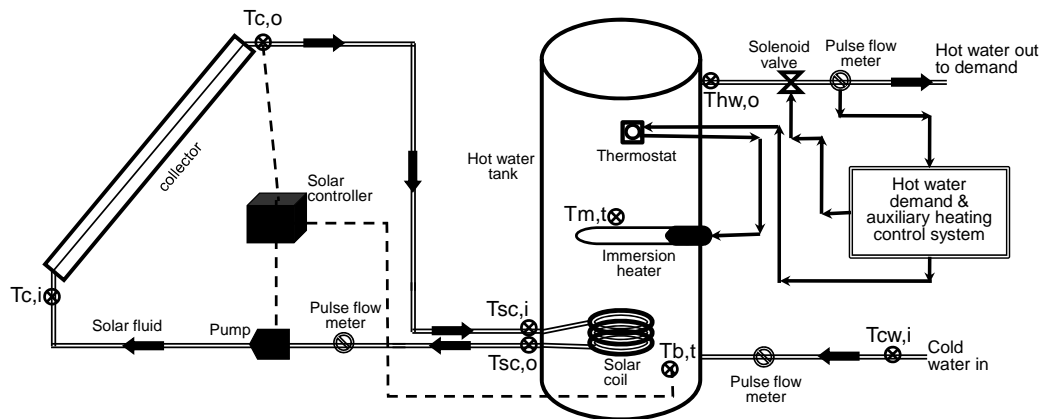
Fig. 4. Schematic diagram of the experimental setup.

2.2 Data measurement and logging

The SWHS was equipped with a RESOL DeltaSol M solar controller which had relay inputs to control the operation of the solar pump station. It also had temperature sensor inputs onto which PT1000 platinum resistance temperature sensors were connected to measure water and solar fluid temperatures (Tc,o-Thw,o) shown in Fig. 3. The volumetric flow rate of the solar fluid was measured using RESOL V40-06 impulse flow meters which react at 1 litre per pulse. RESOL DL2 data loggers were used to store data every minute from the RESOL DeltaSol M solar controllers via RESOL VBus cables. DL2 data loggers were equipped with a secure digital (SD) drive and a local area network (LAN) port for direct connection to a personal computer (PC). Data from the loggers was extracted using a Web browser or an SD card and then converted to text format using the RESOL Service Centre Software.

Global solar radiation on the collector's surface, ambient temperature and wind speed data were measured using a weather station consisting of an SMA Sunny Sensor Box equipped with an ambient temperature sensor and an anemometer. The solar radiation sensor had an accuracy of ±8% and a resolution of 1 W/m^2. The PT1000 platinum temperature sensors had an accuracy of ±0.5°C while the ambient temperature sensor was

a JUMO PT 100 U type with accuracy of ±0.5°C. The anemometer was a Thies small wind transmitter with accuracy of ±5%. Weather data was logged at 5 minute intervals using a Sunny Box WebBox.

3. Energy performance analysis

The energy performance indices evaluated in this study include: energy collected, energy delivered and supply pipe losses, solar fraction, collector efficiency and system efficiency.

3.1. Energy collected

The useful energy collected by the solar energy collector is given as (Kalogirou, 2009):

$$Q_c = \dot{m}C_p(Tc,o - Tc,i) \tag{1}$$

3.2. Energy delivered and supply pipe losses

The useful energy delivered by the solar coil to the hot water tank is given as

$$Q_d = \dot{m}C_p(Tsc,i - Tsc,o) \tag{2}$$

Supply pipe losses were due to the temperature drop as the solar fluid flowed between the collector outlet and the solar coil inlet to the hot water tank. These losses were calculated as:

$$Q_L = \dot{m}C_p(Tsc,i - Tsc,i) \tag{3}$$

3.3. Solar fraction

The solar fraction (SF) is the ratio of solar heat yield to the total energy requirement for water heating and is given as (The German Solar Energy Society, 2007):

$$SF = \frac{Q_s}{Q_s + Q_{aux}} \tag{4}$$

10

3.4. Collector efficiency

The collector efficiency was calculated as (Sukhatme, 1998, Duffie and Beckman, 2006):

$$\eta_c = \frac{\dot{m}C_p(T_{c,o} - T_{c,i})}{A_c G_t} \qquad (5)$$

3.5. System efficiency

The system efficiency was calculated as (Sukhatme, 1998, Duffie and Beckman, 2006):

$$\eta_s = \frac{\dot{m}C_p(T_{sc,i} - T_{sc,o})}{A_c G_t} \qquad (6)$$

4. Results and discussions

4.1. Daily performance

Three days representative of typical weather conditions prevalent in Ireland were used to analyse the daily performance of the HP-ETC SWHS. They consist of heavily overcast sky (28/01/2010), clear sky (04/06/2009) and intermittent cloud covered sky (23/10/2009). Fig. 5 shows plots of solar radiation during the three days. The maximum daily solar radiation was 339.2 Wm^{-2} on the heavily overcast day, 917.2 Wm^{-2} on the clear sky day and 701.3 Wm^{-2} on the day with intermittent cloud cover. Fig. 6 shows plots of ambient air temperature and wind speed. The maximum ambient air temperatures and wind speeds were: 8.5^{o}C and 7.9 ms^{-1} on the heavily overcast day; 22.0^{o}C and 4.5 ms^{-1} on the clear sky day; 15.7^{o}C and 5.1 ms^{-1} on the day with intermittent cloud cover.

11
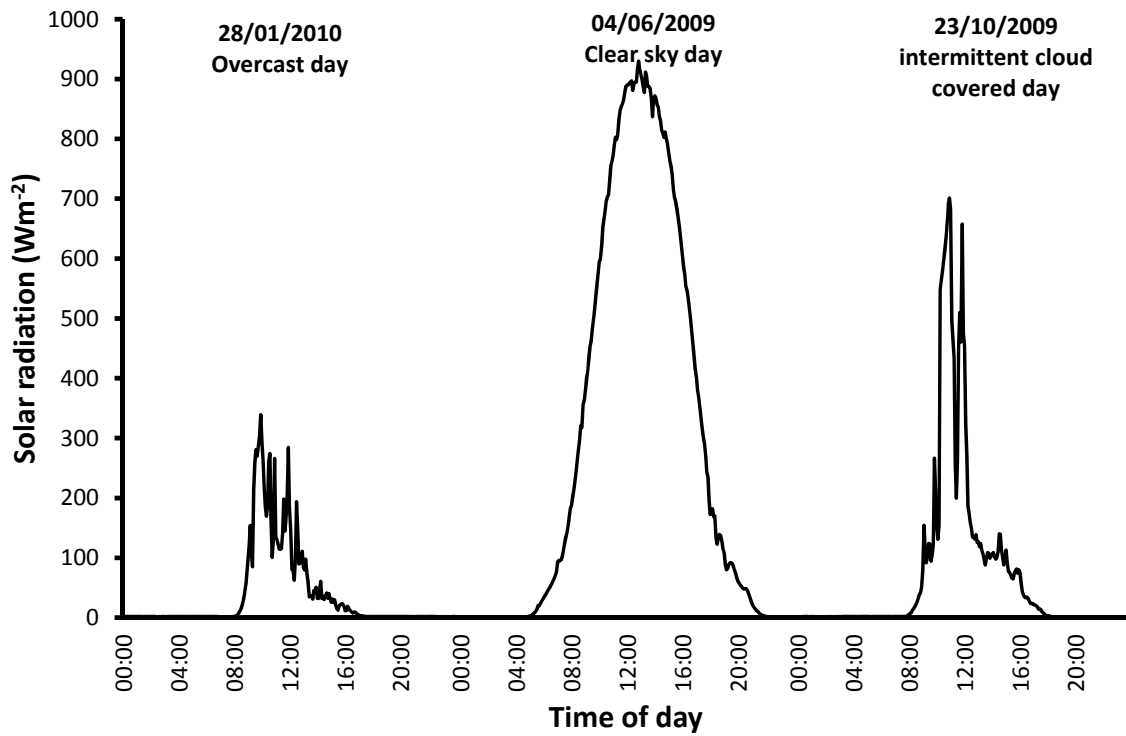
Fig. 5. Global solar radiation on the collector surface for three characteristic days
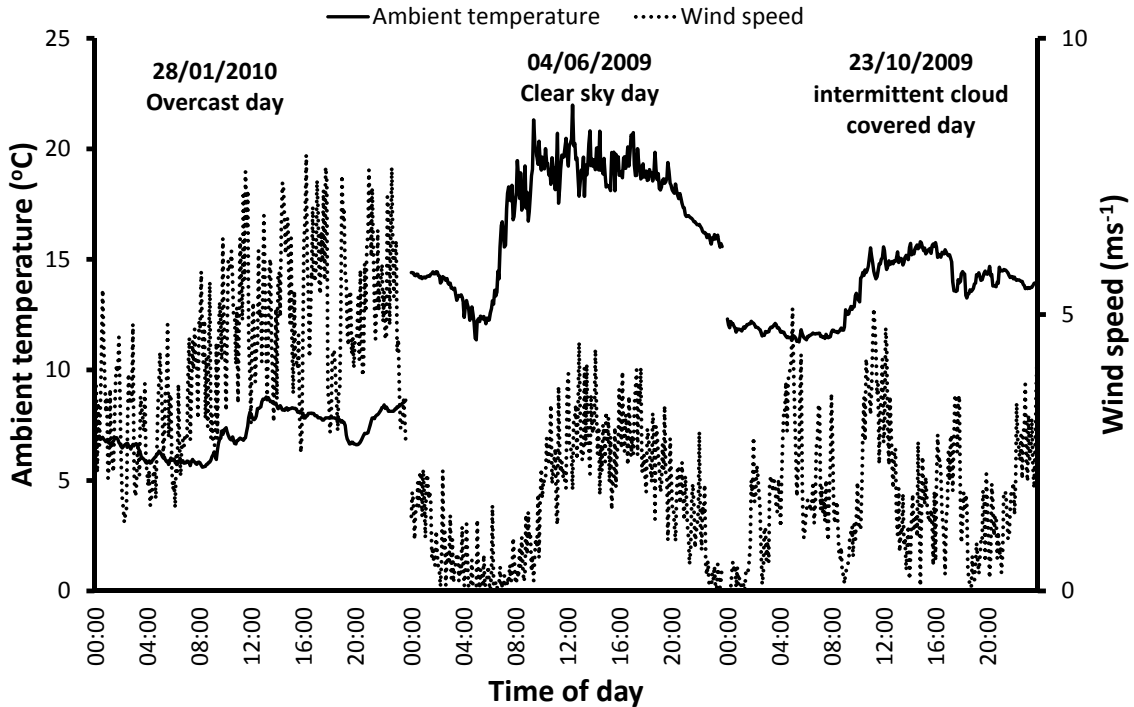
Fig. 6. Ambient air temperature and wind speed for three characteristic days.

4.1.1 System temperatures

Fig. 7 shows plots of daily variation in solar fluid temperature at the collector's outlet ($T_{c,o}$), water temperature at the bottom of the hot water tank ($T_{b,t}$), cold water inlet temperature to the hot water tank ($T_{cw,i}$). It is seen that a rise in $T_{c,o}$ due to solar gain through the collector causes a delayed increase in $T_{b,t}$. The time lag is caused by the time it takes for heat exchange between the solar fluid and water in the tank as well as conduction through the tank fluid to the sensor $T_{b,t}$. Cold water supply was from a tank located in the boiler room of the building on which the experimental rig was installed. Short term variations in $T_{cw,i}$ were as a result of changes in water temperature in the boiler room where the hot water tank was installed.
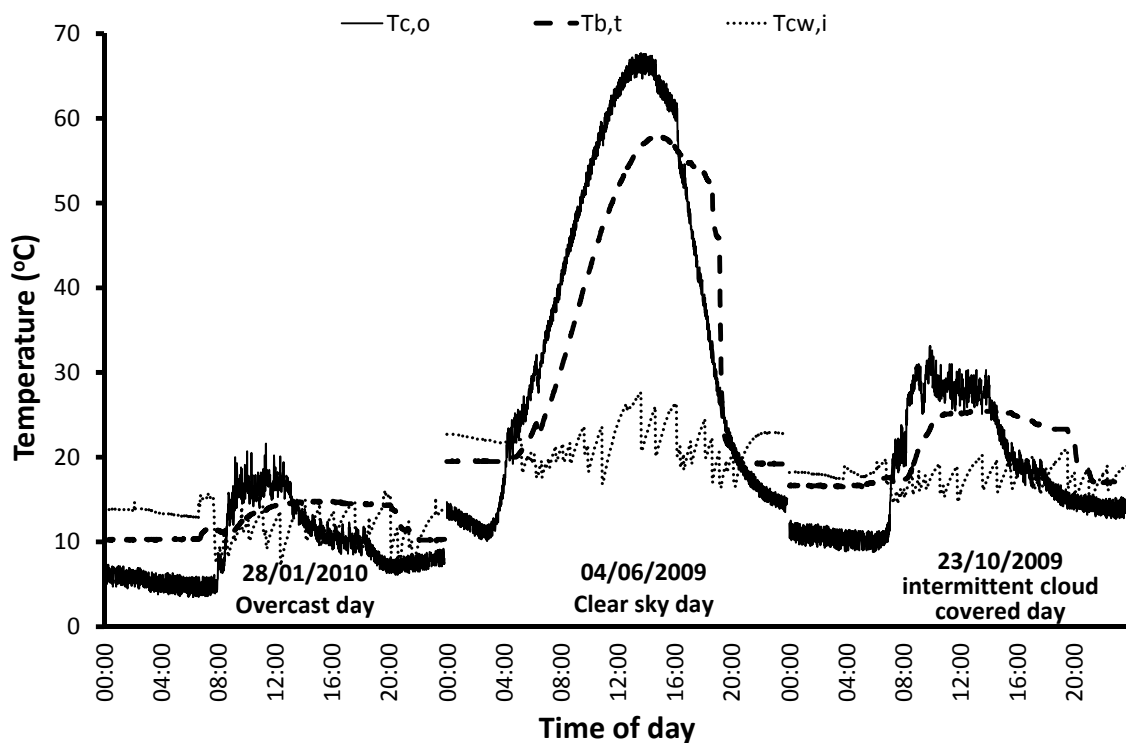
Fig. 7. Daily variation of $T_{c,o}$, $T_{b,t}$ and $T_{cw,i}$.

Fig. 8 shows plots of daily variation of solar fluid temperature at the collector outlet ($T_{c,o}$), water temperature at the bottom of the hot water tank ($T_{b,t}$) and water temperature

at the middle of the hot water tank (Tm,t). It is seen that a rise in Tc,o causes an increase in both Tb,t and Tm,t with both of them lagging behind Tc,o for the same reason explained above. During the heavily overcast and intermittent cloud covered sky days, the immersion heater is called on twice (in the morning and evening) while it is called up only in the morning during the clear sky day since the solar coil raises the water temperature in the tank to the desired level during the daytime period. Tb,t and Tm,t remained very close throughout the heating period with the solar coil during the clear sky day.
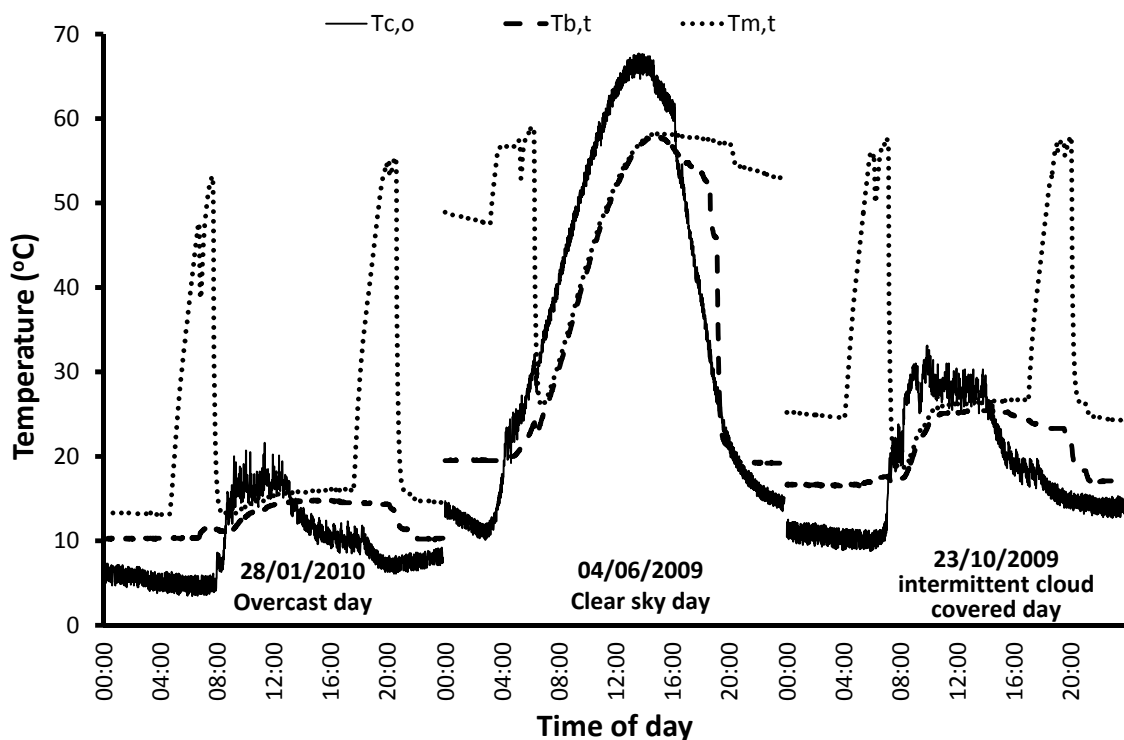
Fig. 8. Daily variation of Tc,o, Tb,t and Tm,t.

Fig. 9 shows plots of daily variation of water temperature at the bottom of the hot water tank (Tb,t), water temperature at the middle of the hot water tank (Tm,t) and hot water supply temperature (Thw,o). Due to difficulties in inserting the thermocouples at the top of the hot water tank, the water temperatures at the top of the tank were considered to be the same as the maximum values of Thw,o measured during hot water draw-offs. It is

seen that during heavily overcast days, $T_{hw,o}$ drops to about $30^{\circ}C$ as water is continuously withdrawn from the tank using the tapping cycle. However, during the clear sky day, $T_{hw,o}$ did not drop below $50^{\circ}C$ due to the relatively greater quantity of heat delivered by the solar coil throughout the day time. This shows that for a continuous stream of clear sky days, the SWHS would provide all the hot water required in the evening with a reduced quantity of auxiliary energy required in the morning.
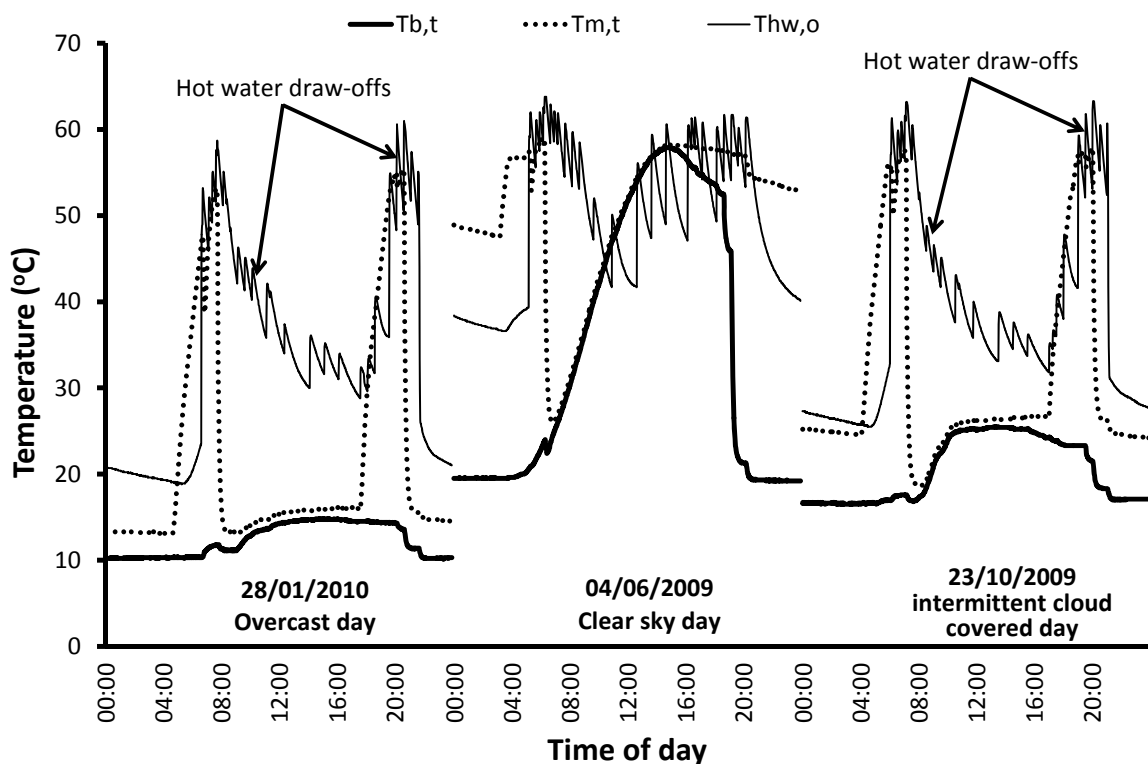
Fig. 9. Daily variation of $T_{b,t}$, $T_{m,t}$ and $T_{hw,o}$.

The immersion heater at the middle of the tank was programmed to switch on between 5-8 am and 6-9 pm daily. An analogue thermostat installed at the top of the tank was used to maintain the water temperature around $60^{\circ}C$. This ensured that hot water was available in the tank when needed to satisfy the largest hot water demands at 7:05 am, 8:05 am, 8:30 pm and 9:00 pm as shown in Fig. 1. The timing was such that there was always enough cold water at the bottom of the hot water tank to be heated by the solar coil during

even on a clear sky day (04/06/2009) when no auxiliary energy was required from the immersion heater in the evening. On the other hand, during a heavily overcast day (28/01/2010) or intermittent cloud covered day (23/10/2009) the immersion heater was used to heat water in the tank both in the morning and evening.

4.1.2. Solar fluid mass flow rate

Fig. 10 shows variation of the solar fluid mass flow rate during the three days. On the heavily overcast day the pump cycled on and off regularly to a peak of 0.167 kgs^{-1} but ran mostly at 0.047 kgs^{-1}. During the clear sky day the pump operated at four different flow rates 0.047, 0.062, 0.092 and 0.167 kgs^{-1}. The flow rate during solar noon was 0.092 kgs^{-1}. During the intermittent cloud covered sky day the pump ran at three different flow rates 0.047, 0.062 and 0.167 kgs^{-1}. Table 1 shows the percentage of time the SWHS pump operated at different flow rates.
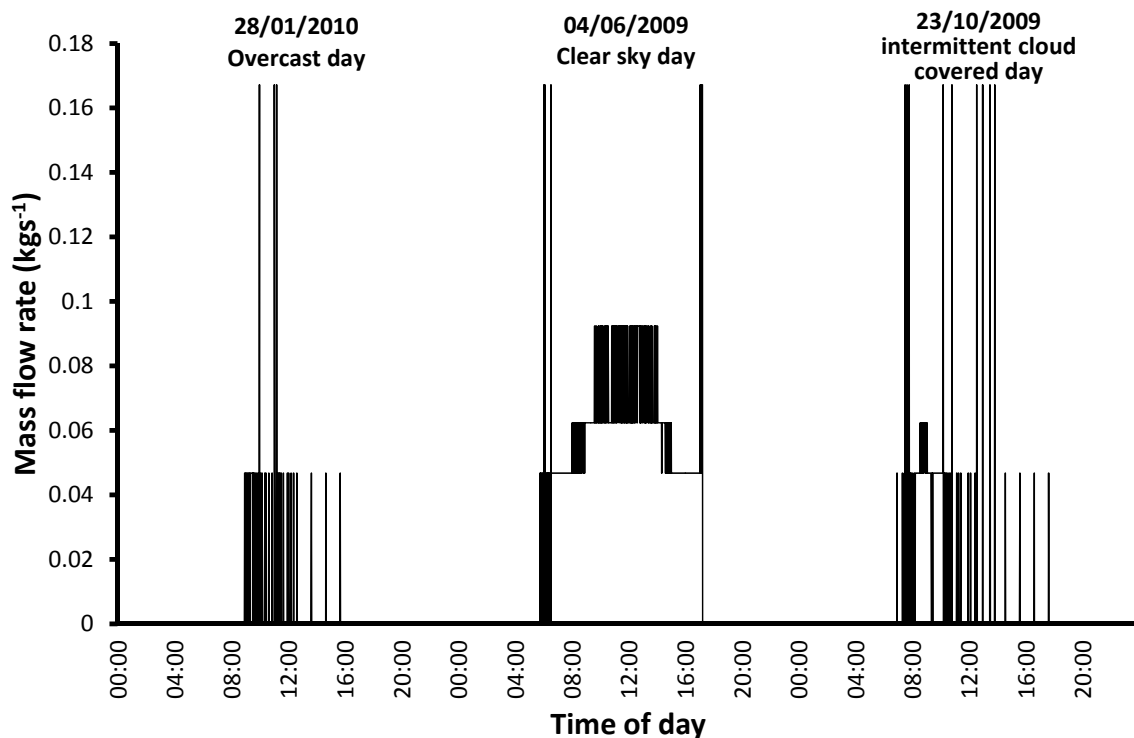
Fig. 10. Solar fluid mass flow rate.

Table 1: Percentage of time the SWHS pump operated at different flow rates

Flow rate (kgs-1)	Percentage (%)		
	Clear sky day (04/06/2009)	Intermittent cloud covered day (23/10/2009)	Overcast day (28/01/2010)
0.047	40.0	82.6	90.0
0.062	38.9	11.4	0.0
0.092	19.8	0.0	0.0
0.167	1.4	6.0	10.0

4.1.3. Energy collected

Fig. 11 shows the energy collected by the HP-ETC system. The total daily energy collected was 187.8 MJ on 28/01/2010, 3,337.4 MJ on 04/06/2009 and 627.5 MJ on 23/10/2009. It can be seen that the system operates even during low levels of solar insolation at sunrise and sunset, and during days characterised by intermittent cloud covered skies. This has an impact on the quantity of energy collected since short intermittent flows of the solar fluid tended to carry heat away from the hot water tank and dump it in the supply line to the collector leading to energy losses as seen in Fig. 11. The resulting energy losses were 5.1 MJ on 28/01/2010, 7.1 MJ on 04/06/2009 and 14.3 MJ on 23/10/2009. This leads to a reduction in the energy collected and, in some periods during the cold winter months to net negative daily energy balances.
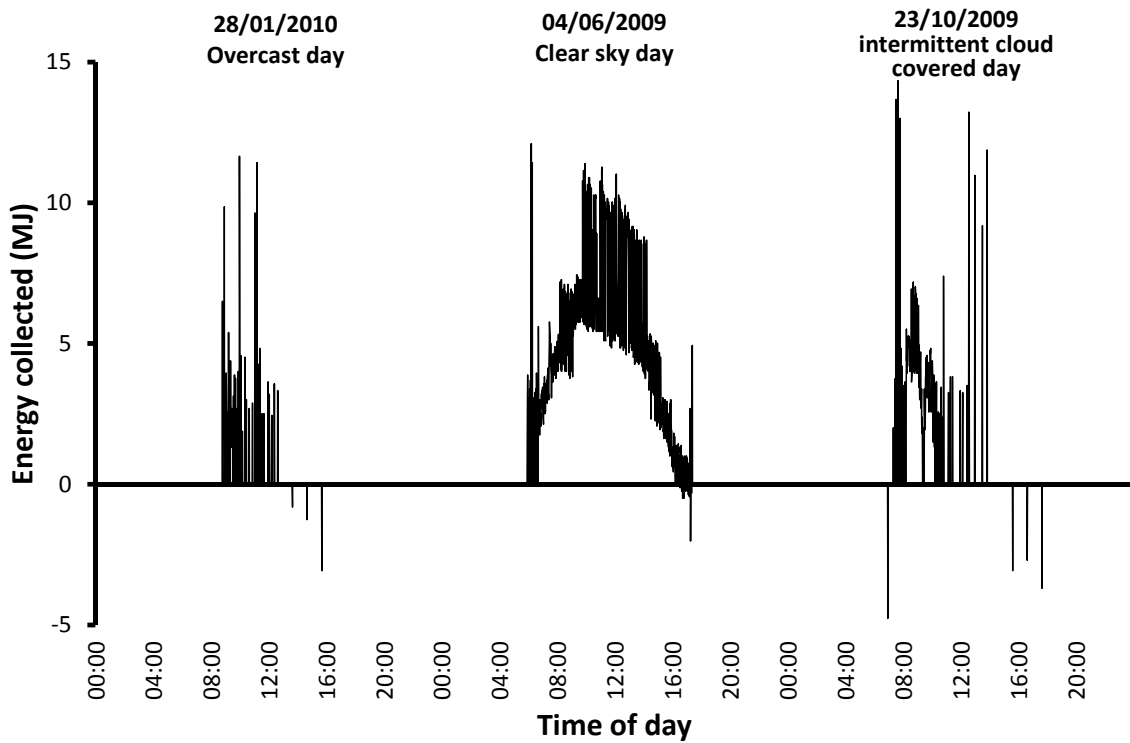
Fig. 11. Energy collected.

4.2. Monthly Performance

4.2.1. System temperatures

Fig. 12 shows maximum recorded monthly water temperatures at $T_{c,o}$, $T_{b,t}$, $T_{m,t}$, $T_{cw,i}$ and $T_{hw,o}$. The maximum monthly water temperatures at $T_{m,t}$ and $T_{hw,o}$ were fairly constant throughout the year around $59.0^{o}C$ and $65^{o}C$. Maximum monthly water temperatures at $T_{c,o}$ varied between $35.9^{o}C$ in December and $70.3^{o}C$ in April, $T_{b,t}$ varied between $26.7^{o}C$ in December and $59.5^{o}C$ in June while $T_{cw,i}$ varied between $18.5^{o}C$ in January and $28.2^{o}C$ in June.

18
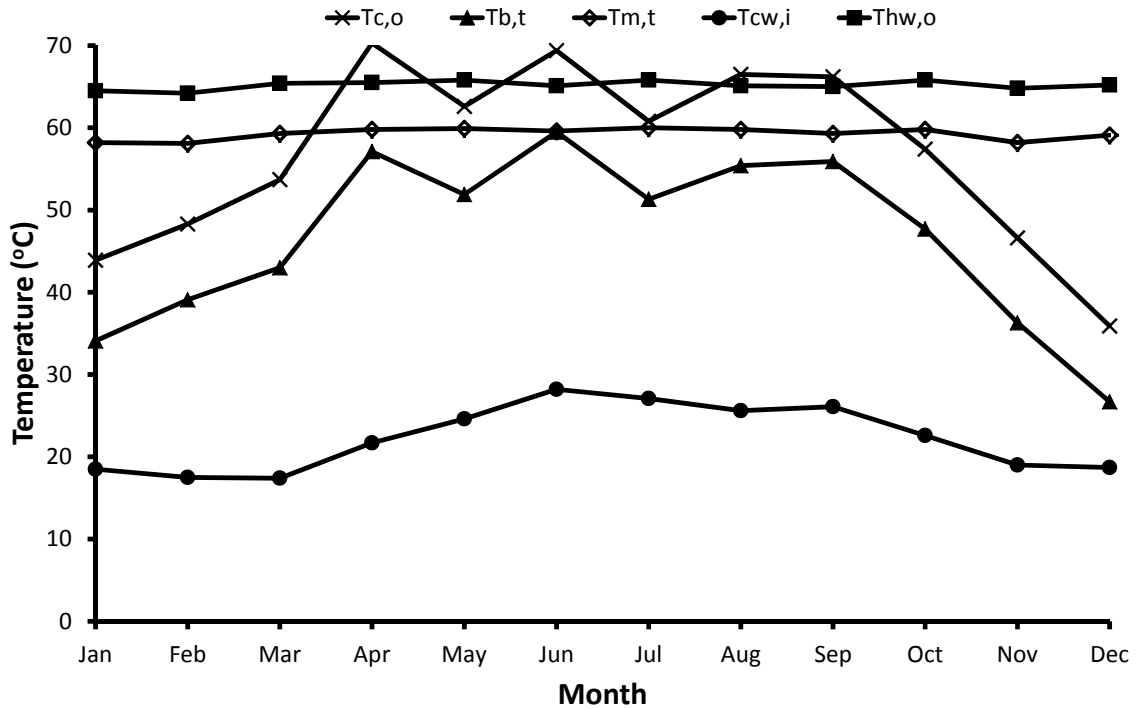
Fig. 12. Maximum monthly water temperatures at Tc,o, Tb,t, Tm,t, Tcw,i and Thw,o.

4.2.2. Energy collected, delivered and losses

Fig. 13 shows monthly and annual average daily global solar insolation on the collector's surface, energy collected and delivered to the hot water tank as well as supply pipe losses. The monthly average daily global solar insolation on the collector's surface varied between 13.0 MJd^{-1} in December and 49.7 MJd^{-1} in June, energy collected varied between 6.1 MJd^{-1} in December and 34.2 MJd^{-1} in June, energy delivered varied between 5.4 MJd^{-1} in December and 27.7 MJd^{-1} in June while supply pipe losses varied between 0.7 MJd^{-1} in December and 6.5 MJd^{-1} in June. Annual average daily solar insolation on the collector's surface was 32.2 MJd^{-1}, energy collected was 20.4 MJd^{-1}, energy delivered was 16.8 MJd^{-1} and supply pipe loss was 3.6 MJd^{-1}.
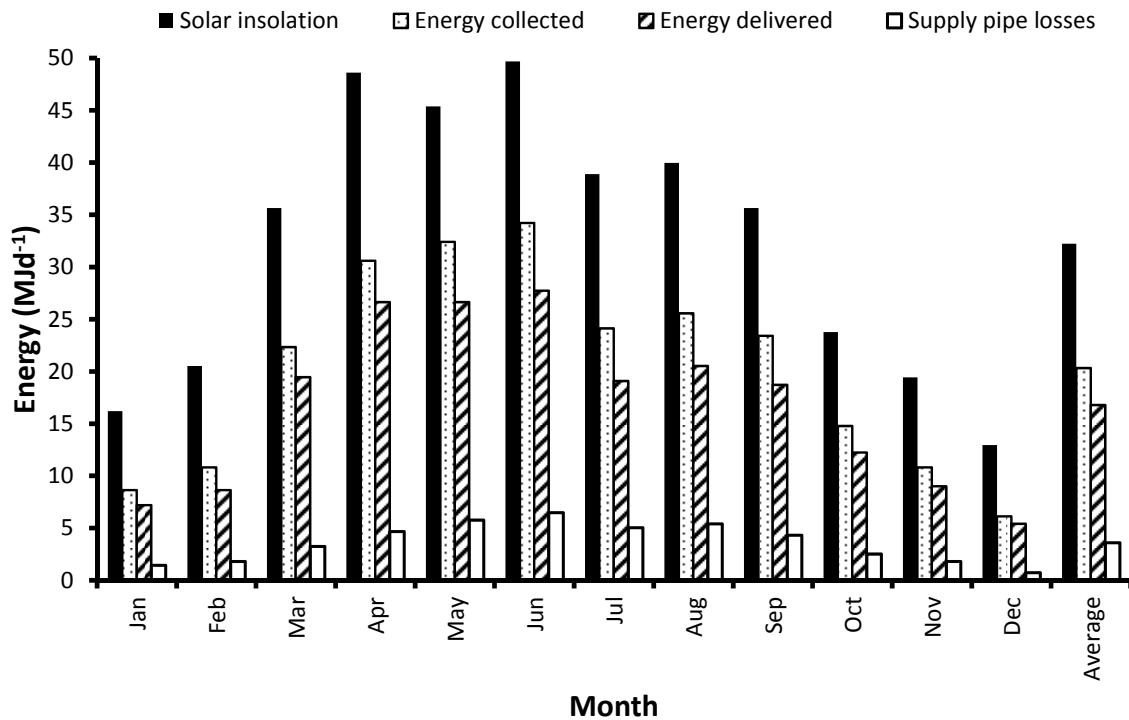
Fig. 13. Monthly and annual average daily global solar insolation on the collector's surface, energy collected, delivered and supply pipe losses.

For an annual global solar insolation on the collector's surface of 11,760.3 MJ, a total of 7,435.1 MJ was collected while 6,121.1 MJ was delivered to the hot water tank. Heat losses along the supply side of the solar circuit occurred especially at high collector outlet temperatures. The total annual supply pipe heat loss for the SWHS was 1,314.0 MJ corresponding to 17.7% of energy collected by the HP-ETC and 21.5% of energy delivered to the hot water tank. The supply pipe length should therefore be kept as short as possible and all joints insulated to reduce heat losses. However, this was not the case for our test rig since the hot water tank was located inside the boiler room of the building on which the HP-ETC was installed.

4.2.3. Energy extracted, auxiliary energy and solar fraction

Fig. 14 shows monthly average daily and annual average energy extracted from the hot water tank, auxiliary energy supplied by the electric immersion to the hot water tank

and solar fraction. The monthly average daily energy extracted varied between 46.4 MJd^{-1} in January and 51.5 MJd^{-1} in April to August. The auxiliary energy varied from 23.4 MJd^{-1} in June to 41.8 MJd^{-1} in December. The solar fraction varied between 11.5% in December and 54.2% in June. The annual average daily energy extracted was 49.6 MJd^{-1}, auxiliary energy was 32.8 MJd^{-1} and solar fraction was 33.8%.
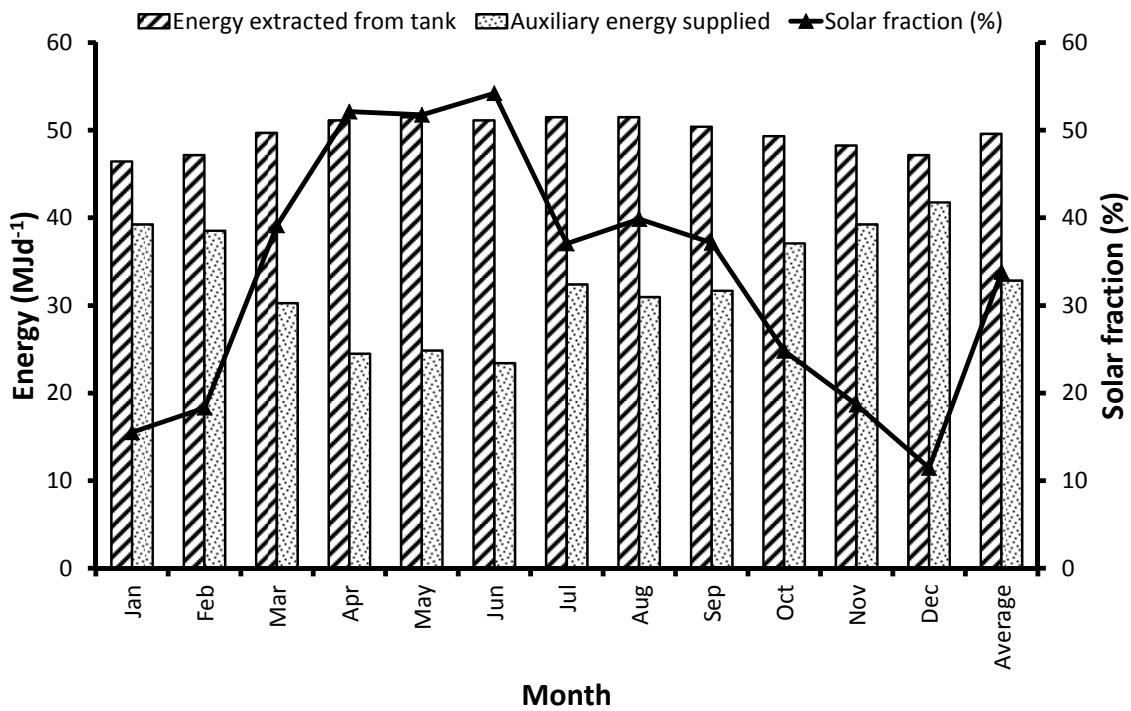
Fig. 14. Energy extracted, auxiliary energy and solar fraction.

4.2.4. Collector and system efficiency

Fig. 15 shows monthly average daily collector and system efficiencies. The average daily collector efficiency varied from 47.2% in December to 71.4% in May while the system efficiency varied from 41.7% in December to 58.7% in May. The annual average daily collector efficiency was 63.0% while the system efficiency was 52.0%.
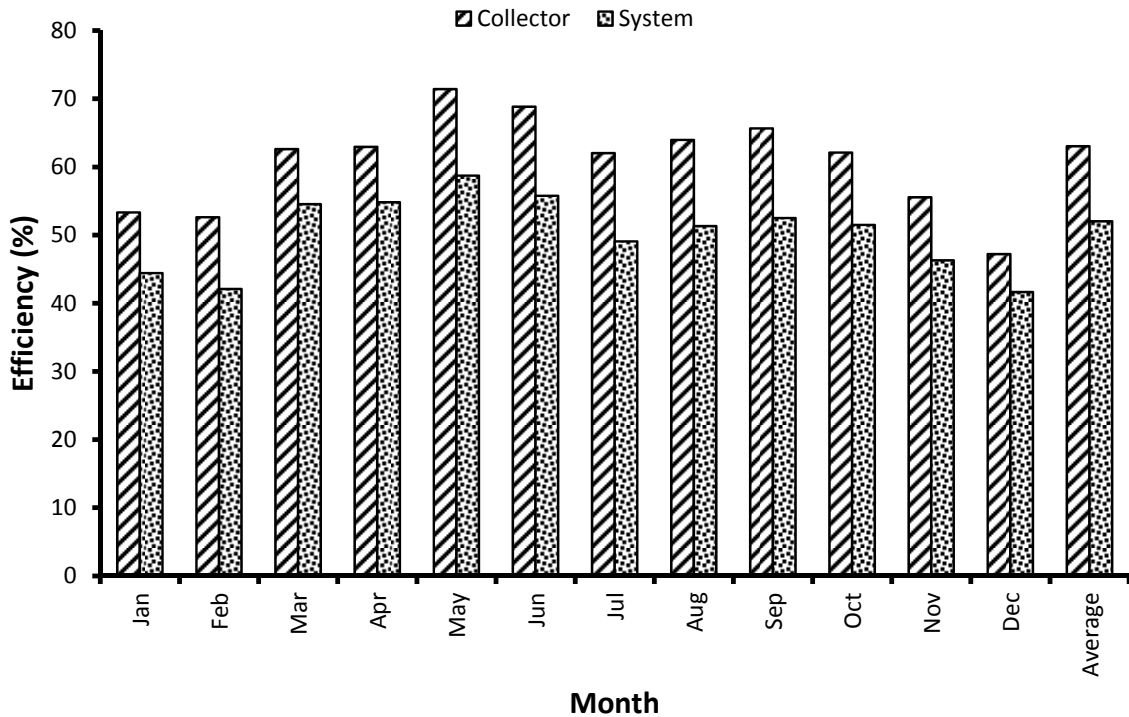
Fig. 15. Monthly average daily collector and system efficiencies.

5.   Conclusions

The year-round energy performance analysis of a commonly installed SWHS with HP-ETC in a temperate climate was carried out using a field trial installation in Dublin, Ireland. The SWHS was designed and operated to mimic real life operation taking into consideration interaction between the HP-ETC, storage tank and users. An immersion heater was used to supply auxiliary energy when the solar coil was unable to raise the tank water temperature to the required temperature.

Results showed that for an annual global solar insolation on the collector surface of 11,760.3 MJ, a total of 7,435.1 MJ was collected while 6,121.1 MJ was delivered to the hot water tank. For 11,973.3 MJ of auxiliary energy supplied to meet the total hot water demand of 18,100.4 MJ, the annual solar fraction was 33.8%. Annual average daily energy collected, energy delivered by the solar coil, supply pipe losses were 20.3 MJd^{-1}, 16.8 MJd^{-1} and 3.6 MJd^{-1} respectively. Annual average solar fraction, collector efficiency and system

efficiency were 33.8%, 63.2% and 52.0% respectively. The maximum recorded collector fluid outlet temperature was 70.3^{o}C while the maximum recorded water temperature at the bottom of the hot water tank was 59.5^{o}C.

The total annual supply pipe heat loss for the SWHS was 1,314.0 MJ corresponding to 17.7% of energy collected by the HP-ETC and 21.5% of energy delivered to the hot water tank. The solar circuit supply pipes should therefore be kept as short as possible in order to reduce energy loss. The low thermal mass of a HP-ETC causes it to absorb solar radiation and transmit heat quickly to the solar fluid. Therefore, during heavily overcast or intermittent cloud covered days, the solar controller would intermittently switch the circulation pump on and off since it operates based on temperature difference between the collector outlet temperature and bottom of the hot water tank. This resulted in an energy loss of 5.1 MJ on 28/01/2010, 7.1 MJ on 04/06/2009 and 14.3 MJ on 23/10/2009. A better pump control strategy for heavily overcast and intermittent cloud covered days could result in an improvement of the HP-ETC SWHS.

A comparison of the results from this study against those from the study carried out by Building Research Establishment (2009) revealed that HP-ETCs would generate 2,478.4 MJm^{-2} while flat plate collectors would generate 1,755.4 MJm^{-2} of heat in northern maritime climates. This shows that HP-ETCs are more efficient than their flat plate counterparts when operating as components of a solar water heating system.

Nomenclature

A_c	collector area (m^2)
C_p	specific heat capacity of solar fluid (Jkg^{-1}K^{-1})
G_t	total global solar radiation on the collector's surface (Wm^{-2})
$\dot{m}$	solar fluid mass flow rate (kgs^{-1})
Q_{aux}	auxiliary heating requirement (MJ)
Q_c	useful heat collected (J)
Q_d	useful heat delivered (J)
Q_l	supply pipe heat loss (J)
Q_s	solar yield (MJ)
SF	solar fraction (%)
η_c	collector efficiency (%)
η_s	system efficiency (%)

References

Building Research Establishment, 2009. Clearline Solar Thermal Test Report – Average Household Simulation, Viridian Solar, Client report number 251175. Available at: http://www.viridiansolar.co.uk/Assets/Files/BRE_Report_Viridian_Solar_Average_House_Simulation.pdf.

Chow, T.T., Dong, Z., Chan, L.S., Fong, K.F., BAI, Y., 2011. Performance evaluation of evacuated tube solar domestic hot water systems in Hong Kong. Energy and Buildings 43, 3467-3474.

de Vries, H.F.W., Kamminga, W., Francken, J.C., 1980. Fluid circulation control in conventional and heat pipe planar solar collectors. Solar Energy 24, 209-213.

Duffie, J.A., Beckman, W.A., 2006. Solar engineering of thermal processes, 3rd ed., Wiley, New Jersey.

Dunn, P.D., Reay, D.A., 1982. Heat pipe, Pergamon Press, New York.

European Commission, 2002. Mandate to CEN and CENELEC for the elaboration and adoption of measurement standards for household appliances: water heaters, hot water storage appliances and water heating systems, Brussels.

Faghri, A., 1995. Heat pipe science, Taylor & Francis, London.

Hayek, M., Assaf, J., Lteif, W., 2011. Experimental Investigation of the Performance of Evacuated-Tube Solar Collectors under Eastern Mediterranean Climatic Conditions. Energy Procedia 6, 618-626.

Houri, A., Salloum, H., Ali, A., Abdel Razik, A.K., Houri, L, 2013. Quantification of energy produced from an evacuated tube water heater in a real setting. Renewable Energy 49, 111-114.

Kalogirou, S.A., 2004. Solar thermal collectors and applications. Progress in Energy and Combustion Science 30, 231-295.

Kalogirou, S.A. 2009. Solar energy engineering: Processes and systems, Elsevier, London.

Morrison, G.L., Budihardjo, I., Behnia, M., 2004. Water-in-glass evacuated tube solar water heaters. Solar Energy 76, 135-140.

Redpath, D.A.G., 2012. Thermosyphon heat-pipe evacuated tube solar water heaters for northern maritime climates. Solar Energy 86, 705-715.

Riffat, S.B., Zhao, X., Doherty, P.S., 2005. Developing a theoretical model to investigate thermal performance of a thin membrane heat-pipe solar collector. Applied Thermal Engineering 25, 899-915.

Sukhatme, S.P., 1998. Solar energy: Principles of thermal collection and storage, Tata McGraw-Hill, New Delhi.

The German Solar Energy Society, 2007. Planning and installing solar thermal systems: A guide for installers, architects and engineers, James and James, UK.

Zambolin, E., Del Col, D., 2010. Experimental analysis of thermal performance of flat plate and evacuated tube solar collectors in stationary standard and daily conditions. Solar Energy 84, 1382-1396.